Optical nanoscopy tools for biologists: advancements of fluorophores and optics for high resolution and live imaging

Dhermendra K. Tiwari[1,*,†], Manisha Tiwari[2,†] and Bikash R. Sahoo[3]

[1]Mechanobiology Institute, National University of Singapore, 5A, Engineering Drive 1, Singapore 117411
[2]RIKEN Quantitative Biology Center, 6-2-3 Furuedai, Suita, Japan
[3]Laboratory of Molecular Biophysics, Institute for Protein Research, Osaka University, Osaka Prefecture 5650871, Japan

Optical nanoscopy has emerged as an important tool for live cell imaging at nanoscale resolution in the field of life sciences. The 2014 Nobel Prize in Chemistry for this invention proves its importance in multidisciplinary areas of science. Several optical nanoscopic methods have been introduced in the past decade to achieve diffraction-unlimited resolution by implementing new optical set-ups or utilization of unique photoswitchable fluorophores, or both. In this review we extensively discuss the biological importance of nanoscopy, and the latest advancements and types of fluorophores needed for imaging. This review will be a starter-kit for biologists working in the field of bioimaging.

Keywords: Fluorophores, live cell imaging, optical nanoscopy, optical set-up.

Background

TO understand intracellular activities in detail, exploration of all their components such as cell activity, molecular interaction, structural insights, molecular dynamics is required. From the very beginning, microscopy-based cellular study played an important role in cell biology[1–7]. Fluorescence bioimaging helped realize many groundbreaking, biologically important discoveries in living systems in several studies such as neurobiology[8], cellular dynamics[9–13], molecular interactions[14,15], biomolecule counting[16–18] and *in vivo* imaging[19–23]. It is well known that fluorescence microscopy can allow imaging different cellular structures labelled with fluorophores with good signal-to-noise ratio and high specificity. This makes fluorescence imaging an indispensable tool in life sciences. However, fluorescence microscopy techniques are limited in their lateral and spatial resolution because of the wave nature of light, which restricts the separation of structures located closer than half the wavelength of light used for imaging[24,25]. This phenomenon is called the diffraction limit of light, and was introduced by Ernest Abbe in 1873. Hence, it is also known as Abbe's rule of diffraction limit.

Abbe's diffraction limit (D) = (λ/2NA)

where λ is the wavelength of light and 'NA' is the numerical aperture of the objective lens.

The light distribution from a focal spot in Fourier space is bigger than the actual size of the fluorescence spot in both x–y and x–z directions. This is because the generated image in the focused image plane consists of fluorescent signals from several points in the specimen, and is represented by the formation of Airy diffraction pattern. The resolution limit criteria given based on closeness of two Airy discs generated from different imaging point sources, is called the Rayleigh criterion[5,25,26] (Figure 1). If the distance between the two Airy disks or point spread function (PSFs) is greater than this value, the two point sources are considered to be resolved (and can readily be distinguished).

Rayleigh resolution = (0.61λ/NA).

Due to the diffraction limit, the penalty for using excitation beam in visible light domain is low spatial resolution. An early and powerful approach to obtain more

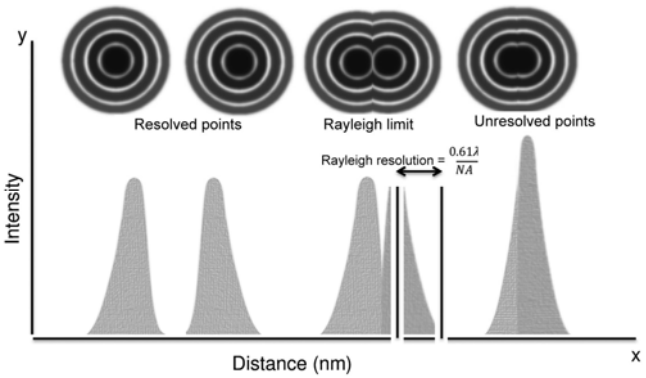

Figure 1. Illustration of lateral resolution of light microscopy explained by Rayleigh limit for two objectives close to each other.

*For correspondence. (e-mail: dhermendratiwari@gmail.com)
†These authors contributed equally.

detailed resolution was the use of electrons instead of photons to form the image. Electron microscopy (EM) achieves 100 times superior resolution than light microscopy due to its relative (i.e. 105 times) smaller wavelength[27,28]. However, both transmission and scanning EM techniques are technically challenging, expensive, less user-friendly and time-consuming. To overcome this challenge, many fluorescence microscopy techniques were invented to achieve spatial resolution far better (30–40 nm) in comparison to the diffraction limit of visible light (>200 nm) (Figure 2). This resolution is not as good as that using EM, but there is scope to constantly improve it at the molecular scale[29,30]. These techniques are collectively known as 'nanoscopy' that has profound impact on biology and other fields in which sub-diffraction-limited resolution of fluorescently labelled samples is desired. Considering the importance of nanoscopy techniques, the 2014 Nobel Prize in Chemistry was awarded to Stefan W. Hell, Eric Betzig and William E. Moerner.

Nanoscopy roughly includes three categories based on the light pattern used: (i) defined illumination pattern-based, (ii) wide-field illumination based and (iii) polarized illumination-based. Popular techniques in the first category are stimulated emission depletion (STED) microscopy[31], reversibly saturable optical fluorescence transition (RESOLFT) microscopy[31], saturated structured illumination (SSIM) microscopy[32], Bessel-beam plane illumination nanoscopy (BBPIN)[33] and lattice light sheet nanoscopy (LLSN)[34]. The second category includes photo-activatable localization microscopy (PALM)[35], direct stochastic switching microscopy (DSSM) and stochastic optical reconstruction microscopy (STORM)[36]. The third and most recent technique based on polarization of light is called super-resolution by polarization demodulation-exactly perpendicular to the polarization of the exciting light (SPoD-ExPan) nanoscopy[37].

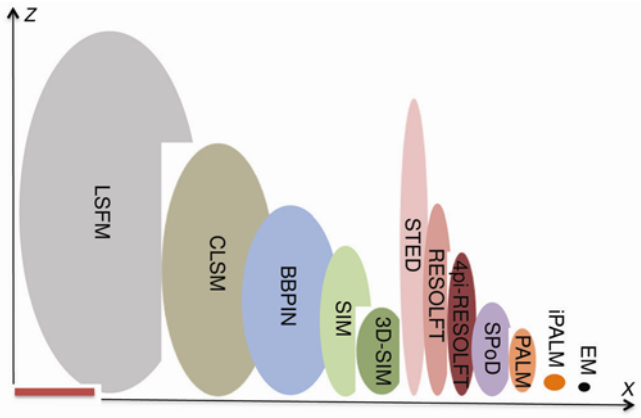

Figure 2. Spatial resolution of optical microscopies in *x*–*z*. Scale bar = 100 μm.

Nanoscopy with defined illumination pattern (STED, RESOLFT, SIM and SSIM)

A direct approach to constrain the fluorescence focal spot to a diffraction unlimited spot consists of a selective reduction of a part of the circumference fluorescence. This simple but powerful concept was used in STED, where the fluorescence was switched using a deterministic nanometric interference pattern of STED beam[31,38]. Increasing the STED pulse intensity erases the fluorescence signal at the periphery of the spot, reducing its size. Ideally, the fluorescence signal will be liable at the centre of the doughnut hole. A modified Abbe's equation describes this sub-diffraction resolution as

$$D = \frac{\lambda}{2n\sin\alpha\sqrt{1+\frac{I}{I_{\text{sat}}}}},$$

where λ is the wavelength, $n\sin\alpha$ the numerical aperture of the microscope, I the applied intensity of the STED pulse and I_{sat} is the STED intensity that gives 50% depletion of the emission[39]. The laser power used for STED beam is strong (>MW) to consider its applicability for live cell study. As reported earlier, strong laser power can cause cell death and photobleaching of the fluorophore; thus the high power is neither useful for live cell imaging nor fixed cell imaging. Hence, the STED nanoscopy is limited to short-time imaging of a photo-insensitive sample.

The more biocompatible version of STED, called RESOLFT, has been implemented with a combination of unique photochromic fluorophores (Figure 3 *a*). RESOLFT is an advanced version of the STED principle utilizing

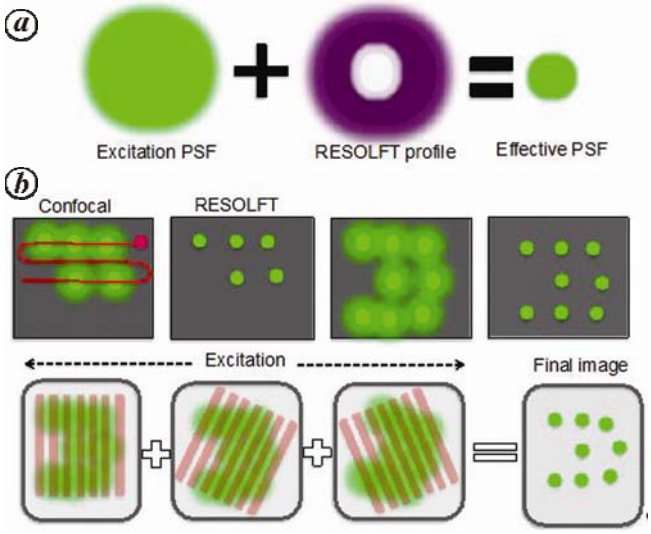

Figure 3. Schematic of the principle of patterned illumination-based super-resolution imaging. ***a***, RESOLFT imaging and ***b***, SSIM imaging.

photoswitchable fluorescent probes rather than a strong STED beam, and allows achieving a resolution (30–40 nm) far better than the diffraction limit of light (>200 nm)[40–42]. In contrast to STED, RESOLFT achieves super-resolution at very low laser power (<10^{-6} times) by altering the point-spread function of ensemble photoswitchable fluorophores. RESOLFT proved its superior in several live cell-imaging studies, attaining a resolution up to ~20 nm (refs 40–44).

SSIM is based on the nonlinearity principle. Here, a sample is illuminated with high-frequency sinusoidal striped light, which can be generated by laser light passing through a movable optical grating and projected via the objective onto the sample[32,45–49] (Figure 3 *b*). However, SSIM usually requires high laser power to achieve nonlinearity for improvement of resolution[32,45,46]. The latest SSIM techniques are now using photochromic fluorophores to achieve nonlinearity at low laser power because the power of light needed for switching them on/off is much lower than that used in conventional SSIM microscopy[21,47,49,50].

Recent addition to defined illumination-based nanoscopy

The above discussed fluorescence nanoscopy techniques used for 3D imaging expose entire samples due to their dependency on epi-illumination optics (wide field, SSIM, 3D-PALM, STED) which compromises with loss of large amounts of fluorescence signal. Especially live cell imaging is hampered due to whole area illumination proceeding to continuous photobleaching. Light sheet fluorescence microscopy (LSFM) has a relatively intermediate optical resolution than the above discussed nanoscopy techniques. It uses a thin sheet of light to optically section the imaged object labelled with a fluorophore. In contrast to other nanoscopy techniques, LSFM only illuminates a very thin section of the imaged object perpendicular to the direction of observation. Several LSFM techniques have been developed with continuous improvement of spatial and temporal resolution. The most recent one, Bessel beam plane illumination microscopy (BBPIM), is based on a thin light sheet illumination that achieves ~300 nm resolution in 3D with a conventional fluorophore[33,51]. BBPIN uses a special Bessel light beam, which has highly non-diffractive property. The resolution of BBPIM could be further improved using photocontrollable or photoswitchable fluorophores. Recently, BBPIM combined together with a structured illumination approach lead to great improvement in resolution (both *x*–*y* and *x*–*z* directions) with reduced phototoxicity. This new nanoscopy approach is known as lattice light sheet nanoscopy (LLSN)[34]. Both BBPIM and LLSN are best suited for long-time 3D imaging with very low phototoxicity.

Nanoscopy with wide-field illumination (PALM, STORM)

In this category, nanoscopy uses the principle based on high-precision localization of a single fluorescence emitter (Figure 4 *a*). To avoid overlapping of adjacent fluorophores, optimum concentration of the fluorescence molecules is necessary. The localized positions of emitting fluorophores from the set of image frames can be combined to yield a nanoscopy image for some defined cellular structure. The Poisson process of photon detection determines the precise localization of the single molecules; thus the most crucial factor is the detected photon from the emitter relative to the background[35,36,52].

Basically, the localization nanoscopy aims to keep a limited number of detectable fluorophores sparsely distributed in each frame for their precise localization in diffraction-limited spots. Hence, the intentional control of the emitting single molecules is the key for these methods. The switching-on of the fluorophore molecules in random or stochastic methods should be controlled so that a small subset of labelled fluorophores switches-on in each frame. This process can be controlled either by repeatedly switching the fluorophore on and off, or by switching the fluorophore on and then bleaching it[53–56]. Using this approach, the achievable resolution in stochastically switching methods is down to 10–20 nm, far better than the diffraction limit of light (~200 nm). This improvement caused much excitement and made the single molecule-based nanoscopy methods popular among researchers that eventually led to the 2014 Nobel Prize in Chemistry. Many types of photoswitchable fluorophores are used in this method, which are reversibly or irreversibly switchable from one fluorescent state to another[2,56,57]. Both photochromic chemical dyes and genetically encoded fluorescent proteins (FPs) can be used, depending on the purpose. FPs are commonly used for live cell nanoscopy; however, with some special tag, dyes can also be used for live cell imaging.

PALM and STORM are widely applicable nanoscopy techniques based on localization precision principles. Other similar methods with different names have been invented such as fluorescence PALM, spectral precision distance measurement, direct STORM, PALM with independent running acquisition, etc.[58–60]. Many cellular events have been explored with high resolution using localization precision microscopy techniques. The localization precision for these methods can be calculated as described earlier using the following equation[61,62]

$$(\sigma^2_{x,y})_m \approx \frac{s^2 + \frac{a^2}{12}}{N_m} + \frac{4\sqrt{\pi}s^3 b_m^2}{aN_m^2},$$

where s is the standard deviation of the PSF, a the pixel size in the image (taking into account the system

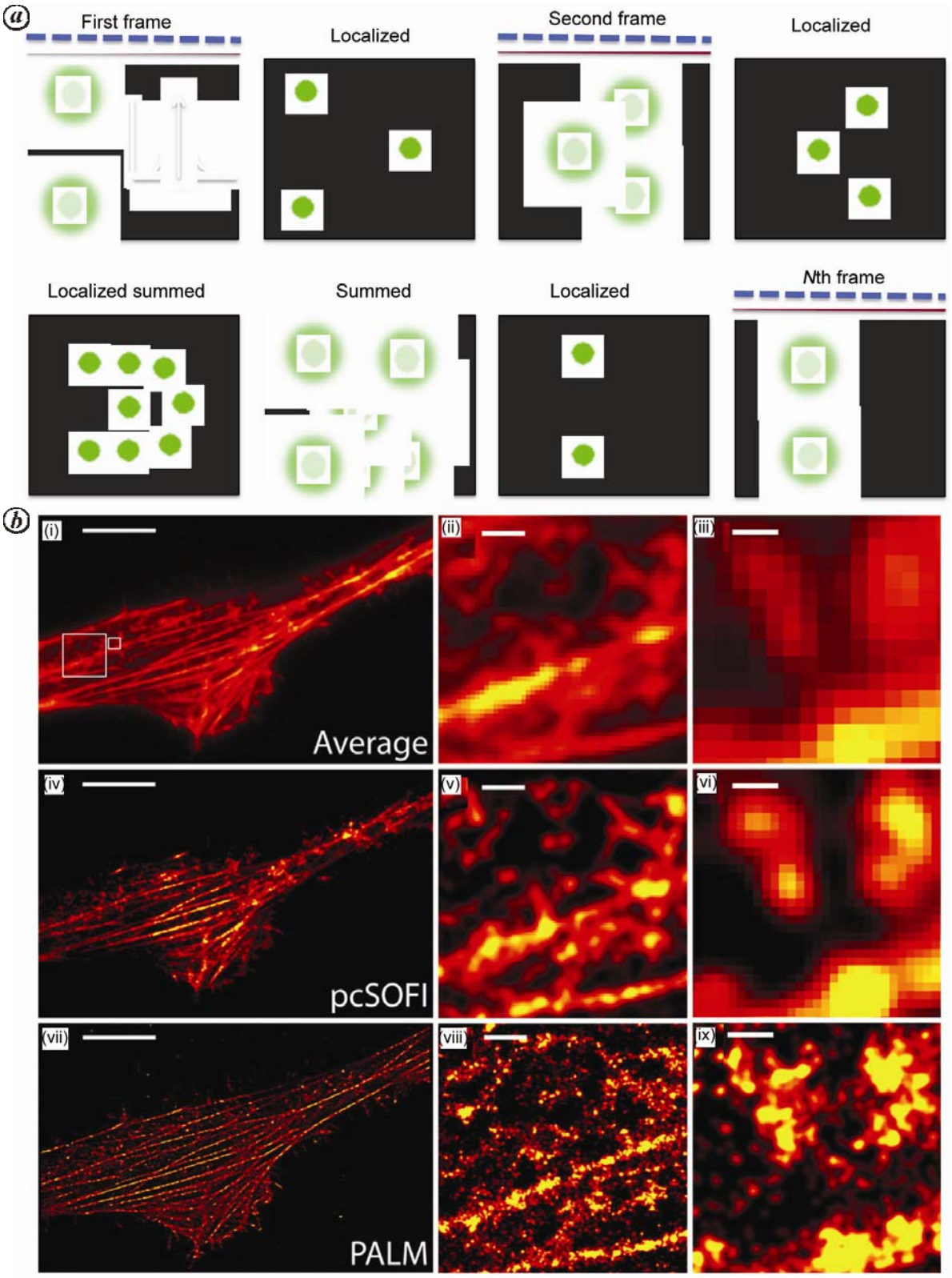

Figure 4. Stochastic blinking-based super-resolution imaging. ***a***, Schematic of PALM imaging principle. ***b***, (i)–(iv) Wide-field image of pcDronpa2-labelled β-actin in HeLa cells made by averaging the 700 frames used in pcSOFI. (v)–(vii) pcSOFI image of the same cell. (viii), (ix) PALM image of the same cell. Scale bar in frames (i), (iv) and (vii) is 10 µm. Frames (ii), (v) and (viii) show details of the β-actin structure (scale bar = 1 µm). Frames (iii), (vi) and (ix) are further zoomed in (scale bar = 0.3 µm). Absence of some actin fibres at the outer edges of the cell in the pcSOFI image is due to the increased *z*-sectioning in pcSOFI combined with imperfections of the 488 nm illumination, and also these structures being slightly out of focus[67].

magnification), N_m the total number of photons measured from molecule m and b_m is the number of background photons collected in the fitting window used for molecule m.

Recent additions in wide-field nanoscopy

pcSOFInanoscopy: Stochastic optical fluctuation imaging (SOFI) is an easy and effective nanoscopy imaging technique that uses blinking signal of fluorophore for reconstruction of nanoscopic images[63]. The extended approach of SOFI in combination with photochromic FPs proteins called photoconversion SOFI or pcSOFI is accessible in live cell nanoscopic imaging with fast and simpler approach[64–66]. A few recently published studies show the potential of pcSOFI for fast, easy and live cell study well below the diffraction limit, using as few as 200–500 image frames for nanoscopic image reconstruction[65,67]. Combination of pcSOFI with reversibly photoswitchable fluorescent proteins (RSFPs) provides robust blinking desired for reconstruction of high-resolution nanoscopic image of pcSOFI (Figure 4 *b*).

Polarization light-based SPoD-ExPAN nanoscopy: Another nanoscopy approach reported recently is based on the polarization of light. The advantage of this approach is that the optical set-up does not require special photocontrollable or photoswitchable fluorophores[68]. This nanoscopy technique is called SPoD and unlike single-molecule detection-based nanoscopy, is applicable to samples with a high density of fluorophores. Polarized excitation used for SPoD allows the collection of signals only from fluorophores with different modulation phases among the fluorophore population. Thus, conventional fluorophores are compatible with this nanoscopy technique. However, the study used another high-power laser exactly perpendicular to the polarization of the exciting light (ExPAN) to further improve resolution[68]. This high laser power could be reduced several hundred-fold using photoswitchable FPs.

Fluorescent proteins for nanoscopy

FPs used in nanoscopy are photocontrollable, i.e. they can either switch between two fluorescent states repeatedly or irreversibly with light irradiation at a certain wavelength. Selection of a suitable PSFP is crucial in nanoscopic imaging. By their photoswitching properties FPs can be categorized as: (i) irreversibly or one-way switching and (ii) reversibly or repeated switching.

One-way switching FPs

In this group, FPs are irreversibly switched from one state to another in response to irradiation (Figure 5 *a* and *b*). Those FPs which are converted from one fluorescent state to another (with a different emission wavelength) receive the name photoconvertable, and the others, which switch from a dark to a fluorescent state are called photoactivatable. Some good examples of one-way photoswitching FPs, which have the ability to switch from the original colour to another red-shifted colour are PAmCherry, mKikGR, PSmOrange, PAtagRFP, PACFP2, mEos2, mEos3 and Dendra2 (Table 1). The commonly used photoactivatable FPs are PA-GFP, PAmRFP1, PAmCherry1, PAmCherry2, and PAmCherry3 (Table 1).

mEos2 (an improved variant of mEosFP) has good folding efficiency, superior spectral properties, high brightness, fast photoconversion and high contrast ratio, making it ideal for fusion tagging for live cell imaging at 37°C. In its thermal equilibrium state mEos2 emits green colour, which can be converted to red state upon violet–blue light irradiation. Several cellular phenomena have been explored using mEos2, such as protein counting within a diffraction-limited region[69], live cell super-resolution imaging of yeast[70], cell tracking, and protein dynamics[71]. However, recently researchers have shown that mEos2 is an oligomer in cells at high concentration[54]. They further engineered mEos2 to develop mEos3.1 and mEos3.2 with truly monomeric nature, high brightness, high photon budget, and fast maturation[54]. Dendra, another green-to-red photoconvertable FP extracted from

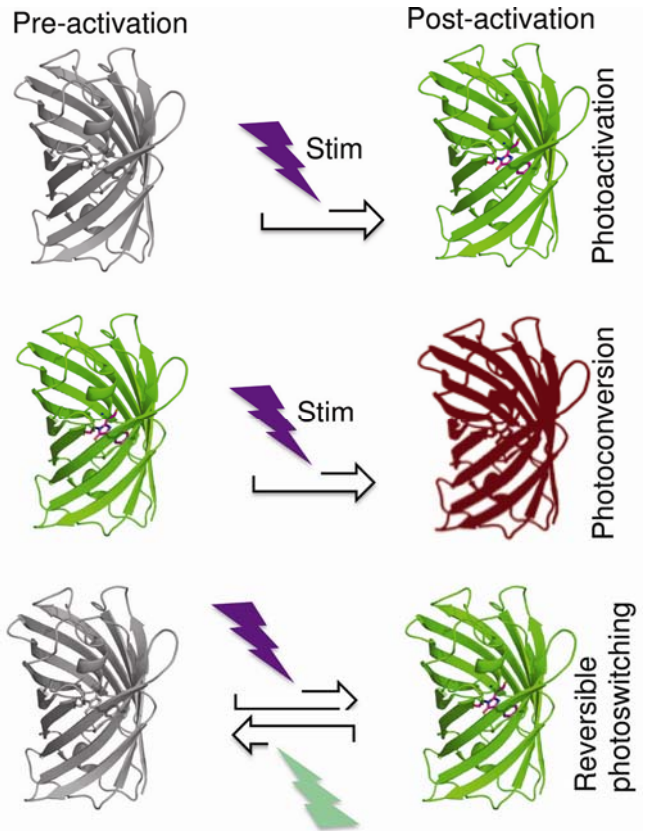

Figure 5. Photoswitching mechanism of fluorescent proteins.

Table 1. PSFPs and their photo-physical characteristics

	Excitation (max), (nm)	Emission (max), (nm)	Excitation coefficient	Oligomeric state	Switching pattern	Light for switching	QY (ON)	Initial colour	Colour change	Chrophorephoto conversion	Application in nanoscopy
mGeos-X	501–506	512–519	51,609–69,630	Monomer	Reversible negative	405/488	0.72–0.85	ON	Dark/green	ND	STORM, PALM, RESOLFT
Dreiklang	515	529	83,000	Monomer	Reversible positive	365/405	0.41	ON	Dark/green	Hydration-Dehydration	STORM, PALM, RESOLFT
Padron	503	522	43,000	Monomer	Reversible positive	488/405	0.64	OFF	Dark/green	Cis-trans conversion	RESOLFT, STORM, SSIM
Dronpa	503	518	125,000	Monomer	Reversible negative	405/488	0.68	ON	Dark/green	Cis-trans conversion	PALM, STORM
psmOrange	548, 636	565, 662	113,300, 32,700	Monomer	Irreversible	Blue–green	0.51, 0.28	Orange	Red	Chromophore oxidation	*In-vivo* imaging, PALM STORM
PSCFP-2	400, 490	468, 511	43,000, 47,000	Monomer	Irreversible	Violet	0.2, 0.23	Cyan	Green	Protonation/ deprotonation	Optical highlighter, PALM, STORM
Kaede	508, 572	518, 582	98,800, 60,400	Tetramer	Irreversible	Violet	0.80, 0.33	Green	Red	pi-conjugation	Optical highlighter, PALM, STORM
mKikGR	505, 580	515, 591	49,000, 28,000	Monomer	Irreversible	UV–violet	0.69, 0.63	Green	Red	Protonation/ deprotonation	Optical highlighter, PALM, STORM
Dendra2	490, 553	507, 573	45,000, 35,000	Monomer	Irreversible	UV–violet	0.5, 0.55	Green	Red	π-Conjugation	Optical highlighter, PALM, STORM

(*Contd*)

Table 1. (*Contd*)

	Excitation (max), (nm)	Emission (max), (nm)	Excitation coefficient	Oligomeric state	Switching pattern	Light for switching	QY (ON)	Initial colour	Colour change	Chrophorephoto conversion	Application in nanoscopy
mEos2	506, 573	519, 584	56,000, 46,000	Monomer	Irreversible	UV	0.84, 0.66	Green	Red	π-conjugation	PALM, STORM, RESOLFT,
mEos3	503, 570	513, 580	88,400, 33,500	Monomer	Irreversible	UV	0.83, 0.62	Green	Red	π-Conjugation	PALM, STORM, RESOLFT
PAmCherry1	564	595	6,500, 18,000	Monomer	Irreversible	Violet	0.46	Dark	Red	Anionic formation of chromophore	PALMIRA, STORM
PAmCherry2	570	596	1,900, 24,000	Monomer	Irreversible	Violet	0.53	Dark	Red	Anionic formation of chromophore	PALMIRA, SPALM, STORM
PAmCherry3	570	596	6,500, 2,1000	Monomer	Irreversible	Violet	0.24	Dark	Red	Anionic formation of chromophore	PALMIRA, SPALM, STORM
PAGFP	504	517	ND	Monomer	Irreversible	Violet	ND	Dark	Green	Protonation/ deprotonation	PALM, STORM
KFP1	580	600	59,000	Tetramer	Irreversible	530	0.07	Dark	Red		STED, SIM, PALM, STORM
PAmRFP1	578	605	10,000	Monomer	Irreversible	Violet	0.08	Dark	Red	Anionic formation of chromophore	PALM, STORM

Octocoral dendronephthya[72] is the only one that uses cyan light (480 nm) for photo conversion. The monomeric Dendra2 has been already developed with improved maturation and brightness[73]. Several super-resolution imaging studies have been made using Dendra2, e.g. vesicle tracking in neuronal gap junctions[74], protein tracking using fluorescence imaging with 1 nm accuracy (i.e. FIONA) in *Caenorhabditis elegans*[75], neuronal branching studies[76], and multi-compartment protein trafficking studies in live cells[77].

Most of the photo-convertable FPs change from green to red emission states. PSCFP2 is the only available Ir-PSFPs that converts from cyan to green[78]. Its initial and photo-convertable states have completely distinct excitation (excitation (ex.) max 468 and 511 nm respectively) and emission spectra (emission (em.) max 400 versus 490 nm respectively). This property of PSCFP2 makes it useful for multi-colour imaging with other photoconvertable or photoswitchable FPs[55,79]. Another photoconvertable FP, PSmOrange and its variant PSmOrange2 have great value in imaging because both FPs have initially orange state (ex. max 548 nm and em. max 565 nm), and upon blue-light excitation can be switched to far-red (ex. max 636 nm and em. max 662 nm). These are the only most far-red-excitable photoconvertable FPs that makes them especially useful for *in vivo* imaging and multi-colour super-resolution imaging[80].

PA-GFP was the first photoactivatable protein developed from wild-type GFP. PA-GFP has a green emission and is used in many studies like protein diffusion, single-cell tracking, protein dynamics study, and neuronal dynamics and developmental studies. Among the red photoconvertable FPs, PAmCherry1 and PATagRFP are the best with QY (0.46 and 0.38 respectively), superior contrast ratio, excellent photostability, fast photoactivation, fast maturation, more suitable pH stability, and monomeric nature that make them ideal for nanoscopy imaging[81,82]. These FPs have proven well for both dual- and triple-colour super-resolution imaging of thick samples in two- and three-dimensional imaging[82,83].

Repeatedly photoswitchable FPs

This group of FPs called reversibly photoswitchable fluorescent proteins (RSFPs) can be switched on/off repeatedly upon UV light irradiation (Figure 5 *c*). Repeated photoswitching of RSFPs is useful for stochastic switching-based super-resolution imaging (e.g. PALM, STORM) and defined illumination-based RESOLFT imaging. Several RSFPs have been developed either from natural sources or by improvement of the existing FPs, e.g. Dronpa, rsFastLime, broad-spectrum Dronpa (bsDronpa), Padron, rsCherryRev, rsCherry, rsEGFP, rsEGFP2, Dreiklang, mGeosXandrsKame (Table 1). Almost all RSFPs show *cis–trans* isomerization during switching, but Dreiklang has a unique switching mechanism based on hydrolysis/dehydration.

Dronpa was the first discovered RSFP with on/off repetition between dark and bright states upon illumination 405 and 488 nm light with very high QY (0.68) and extinction coefficient (98,000 M^{-1} cm^{-1})[84]. Several other Dronpa variants have been developed, namely bsDronpa (broad absorption-Dronpa, with a large Stork shift: abs. max 460 nm and em. max 504 nm), Padron (with a positive photoswitching behaviour), rsFastlime, and pcDronpa (photochromic Dronpa)[42,67]. Padron is unique among all RSFPs because of its positive-switching behaviour. Padron together with other negative switching RSFPs has the potential for dual-label imaging. Dronpa and its variant were used in several super-resolution imaging studies, e.g. cellular dynamics[51], dual-colour and 3D PALM imaging[55] and photochromic stochastic optical fluctuation imaging (pcSOFI)[65,67]. EGFP-based RSFPs (rsEGFP and rsEGFP2) were the first with fast switching speed and large number of switching cycles[39,41]. Both can be repeatedly switched on/off upon illumination with 405 and 491 nm light. Both these RSFPs have proven well in RESOLFT imaging for data storage, rewriting and live cell dynamics tracking.

rsCherryRev, rsCherry and rsTagRFP are red-emitting RSFPs[85,86]. However, the main drawbacks of rsCherryRev and rsCherry are their relatively high residual fluorescence and low brightness, perturbing super-resolution imaging. rsTagRFP is relatively brighter than both rsCherryRev and rsCherry, potentially making it a good partner for green PSFPs in nanoscopy imaging. rsTagRFP switches under blue and yellow light irradiation into a red fluorescent on state and a dark off state respectively. The available number of colour variants of RSFPs is limited; therefore, their development offers many opportunities.

Dreiklang is another unique RSFP that can be switched on and off with 365 and 405 nm light respectively[43], and uses another decoupled light (515 nm) from on/off for

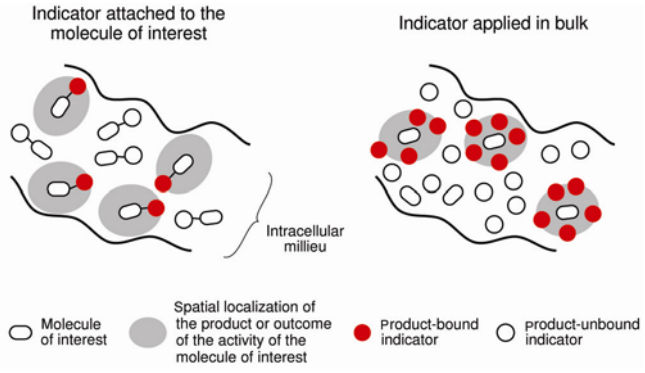

Figure 6. Schematic on the use of photocontrollable indicator for super-resolution imaging.

fluorophore excitation. Dreiklang displays a bright fluorescent equilibrium state (QY 0.41 and extinction coefficient 83,000 M^{-1} cm^{-1}). Padron is better than Dreiklang owing to its high QY (0.64), but the extinction coefficient is nearly half (43,000 M^{-1} cm^{-1}) that of the latter[42]. Given its monomeric nature, Dreiklang is an ideal candidate for fusion tagging in live-cell imaging, allowing to achieve images with a resolution of up to ~35 nm (Figure 6)[43]. The only drawback with Dreiklang is the requirement of three laser lines in the microscopy system. A complete switching cycle for Dreiklang requires excess UV light, which always causes difficulty for live cell imaging. Compared to negative-switching rsEGFP (~1200 cycles), Dreiklang produces just one-tenth of the switching cycles, but its positive-switching characteristics are useful for time-lapse imaging super-resolution imaging. Negative switching R-PSFPs use similar wavelength for both excitation and off-switching; thus they are partially turned-off during excitation. To maintain the signal/noise ratio, high excitation power is required than that desired for excitation, which always causes photobleaching. Both rsEGFP and Dreiklang have homologies similar to that of GFP; therefore, the improvement in the switching cycle of Dreiklang is strongly advocated.

Conclusion

Nanoscopic techniques such as STORM, PALM, RESOLFT, SSIM and SOFI are capable of providing nanoscale resolution. All these techniques utilize photoswitching properties of fluorophores; therefore, the suitable fluorophores are the key factors for nanoscopic imaging. It is crucial to understand chemical structure and photoswitching chemistry for the development of new photoswitchable FPs and their colour variants. PSFPs with multi-colour variants will provide several options for multi-colour super-resolution imaging.

1. Giepmans, B. N. G., Bridging fluorescence microscopy and electron microscopy. *Histochem. Cell Biol*., 2008, **130**, 211–217.
2. Schermelleh, L., Heintzmann, R. and Leonhardt, H., A guide to super-resolution fluorescence microscopy. *J. Cell Biol*., 2010, **190**, 165–175.
3. Ntziachristos, V., Going deeper than microscopy: the optical imaging frontier in biology. *Nature Methods*, 2010, **7**, 603–614.
4. Stelzer, E. H., Wacker, I. and De Mey, J. R., Confocal fluorescence microscopy in modern cell biology. *Semin. Cell Biol*., 1991, **2**, 145–152.
5. Lichtman, J. W. and Conchello, J.-A., Fluorescence microscopy. *Nature Methods*, **2**, 2005, 910–919.
6. Axelrod, D., Total internal reflection fluorescence microscopy in cell biology. *Meth. Enzymol*., 2003, **361**, 1–33.
7. Koster, A. J. and Klumperman, J., Electron microscopy in cell biology: integrating structure and function. *Nature Rev. Mol. Cell Biol.* (*Suppl.*), 2003, SS6–S10.
8. Taraska, J. W. and Zagotta, W. N., Fluorescence applications in molecular neurobiology. *Neuron*, 2010, **66**, 170–189.
9. Klonis, N. *et al.*, Fluorescence photobleaching analysis for the study of cellular dynamics. *Eur. Biophys. J. Biophys. Lett.*, 2002, **31**, 36–51.
10. Klonis, Melanie Rug, Ian Harper, Ma, N. Fluorescence photobleaching analysis for the study of cellular dynamics. *Eur. Biophys. J*., 2002, **31**, 36–51.
11. Haupts, U., Maiti, S., Schwille, P. and Webb, W. W., Dynamics of fluorescence fluctuations in green fluorescent protein observed by fluorescence correlation spectroscopy. *Proc. Natl. Acad. Sci. USA*, 1998, **95**, 13573–13578.
12. Komatsu, T. *et al.*, Real-time measurements of protein dynamics using fluorescence activation-coupled protein labeling method. *J. Am. Chem. Soc*., 2011, **133**, 6745–6751.
13. Michalet, X., Weiss, S. and Jäger, M., Single-molecule fluorescence studies of protein folding and conformational dynamics. *Chem. Rev*., 2006, **106**, 1785–1813.
14. Moerke, N. J., Fluorescence polarization (FP) assays for monitoring peptide–protein or nucleic acid–protein binding. *Curr. Protoc. Chem. Biol*., 2009, **1**, 1–15.
15. Kerppola, T. K., Visualization of molecular interactions by fluorescence complementation. *Nature Rev. Mol. Cell Biol*., 2006, **7**, 449–456.
16. Shu, D., Zhang, H., Jin, J. and Guo, P., Counting of six pRNAs of phi29 DNA-packaging motor with customized single-molecule dual-view system. *EMBO J*., 2007, **26**, 527–537.
17. Vukojevic, V. *et al.*, Quantitative single-molecule imaging by confocal laser scanning microscopy. *Proc. Natl. Acad. Sci. USA*, 2008, **105**, 18176–18181.
18. Renz, M., Daniels, B. R., Vamosi, G., Arias, I. M. and Lippincott-Schwartz, J., PNAS plus: plasticity of the asialoglycoprotein receptor deciphered by ensemble FRET imaging and single-molecule counting PALM imaging. *Proc. Natl. Acad. Sci. USA*, 2012, **109**, E2989–E2997.
19. Filonov, G. S. *et al.*, Bright and stable near-infrared fluorescent protein for *in vivo* imaging. *Nature Biotechnol*., 2011, **29**, 757–761.
20. Chudakov, D. M., Lukyanov, S. and Lukyanov, K. A., Fluorescent proteins as a toolkit for *in vivo* imaging. *Trends Biotechnol*., 2005, **23**, 605–613.
21. Hoffman, R. M. Recent advances on *in vivo* imaging with fluorescent proteins. *Methods Cell Biol*., 2008, **85**, 485–495.
22. Shcherbo, D. *et al*., Bright far-red fluorescent protein for whole-body imaging. *Nature Methods*, 2007, **4**, 741–746.
23. Smith, A. M., Mancini, M. C. and Nie, S., Bioimaging: second window for *in vivo* imaging. *Nature Nanotechnol*., 2009, **4**, 710–711.
24. Zheludev, N. I., What diffraction limit? *Nature Mater.*, 2008, **7**, 420–422.
25. Editorial, Beyond the diffraction limit. *Nature Photonics*, 2009, **3**, 361.
26. Young, A. T., Rayleigh scattering. *Phys. Today*, 1982, **35**, 42–48.
27. Urban, K. W., Is science prepared for atomic-resolution electron microscopy? *Nature Mater*., 2009, **8**, 260–262.
28. Subramaniam, S. and Milne, J. L. S., Three-dimensional electron microscopy at molecular resolution. *Annu. Rev. Biophys. Biomol. Struct*., 2004, **33**, 141–155.
29. Szymborska, A. *et al.*, Nuclear pore scaffold structure analyzed by super-resolution microscopy and particle averaging. *Science*, 2013, **341**, 655–658.
30. Dani, A., Huang, B., Bergan, J., Dulac, C. and Zhuang, X., Superresolution imaging of chemical synapses in the brain. *Neuron*, 2010, **68**, 843–856.
31. Klar, T. A., Jakobs, S., Dyba, M., Egner, A. and Hell, S. W., Fluorescence microscopy with diffraction resolution barrier broken by stimulated emission. *Proc. Natl. Acad. Sci. USA*, 2000, **97**, 8206–8210.
32. Heintzmann, R., Jovin, T. M. and Cremer, C., Saturated patterned excitation microscopy – a concept for optical resolution improvement. *J. Opt. Soc. Am. A*, 2002, **19**, 1599–1609.

33. Planchon, T. A. *et al.*, Rapid three-dimensional isotropic imaging of living cells using Bessel beam plane illumination. *Nature Methods*, 2011, **8**, 417–423.
34. Chen, B.-C. *et al.*, Lattice light-sheet microscopy: imaging molecules to embryos at high spatiotemporal resolution. *Science*, 2014, **346**, 1257998.
35. Betzig, E. *et al.*, Imaging intracellular fluorescent proteins at nanometer resolution. *Science*, 2006, **313**, 1642–1645.
36. Rust, M. J., Bates, M. and Zhuang, X., Sub-diffraction-limit imaging by stochastic optical reconstruction microscopy (STORM). *Nature Methods*, 2006, **3**, 793–795.
37. Hafi, N. *et al.*, Fluorescence nanoscopy by polarization modulation and polarization angle narrowing. *Nature Methods*, 2014, **11**, 579–584.
38. Hell, S. W. and Wichmann, J., Breaking the diffraction resolution limit by stimulated emission: stimulated-emission–depletion fluorescence microscopy. *Opt. Lett.*, 1994, **19**, 780–782.
39. Donnert, G. *et al*., Macromolecular-scale resolution in biological fluorescence microscopy. *Proc. Natl. Acad. Sci. USA*, 2006, **103**, 11440–11445.
40. Grotjohann, T. *et al*., rsEGFP2 enables fast RESOLFT nanoscopy of living cells. *Elife*, 2012, **1**, e00248.
41. Chmyrov, A. *et al.*, Nanoscopy with more than 100,000 'doughnuts'. *Nature Meth.*, 2013, **10**, 737–740.
42. Grotjohann, T. *et al*., Diffraction-unlimited all-optical imaging and writing with a photochromic GFP. *Nature*, 2011, **478**, 204–208.
43. Andresen, M. *et al*., Photoswitchable fluorescent proteins enable monochromatic multilabel imaging and dual colour fluorescence nanoscopy. *Nature Biotechnol*., 2008, **26**, 1035–1040.
44. Brakemann, T. *et al.*, A reversibly photoswitchable GFP-like protein with fluorescence excitation decoupled from switching. *Nature Biotechnol*., 2011, **29**, 942–947.
45. Gustafsson, M. G. L., Surpassing the lateral resolution limit by a factor of two using structured illumination microscopy. *J. Microsc*., 2000, **198**, 82–87.
46. Gustafsson, M. G., Extended resolution fluorescence microscopy. *Curr. Opin. Struct. Biol*., 1999, **9**, 627–634.
47. Hirvonen, L. M., Wicker, K., Mandula, O. and Heintzmann, R. Structured illumination microscopy of a living cell. *Eur. Biophys. J.*, 2009, **38**, 807–812.
48. Mudry, E. *et al.*, Structured illumination microscopy using unknown speckle patterns. *Nature Photonics*, 2012, **6**, 312–315.
49. Shao, L., Kner, P., Rego, E. H. and Gustafsson, M. G. L., Super-resolution 3D microscopy of live whole cells using structured illumination. *Nature Methods*, 2011, **8**, 1044–1046.
50. Rego, E. H. *et al.*, Nonlinear structured-illumination microscopy with a photoswitchable protein reveals cellular structures at 50-nm resolution. *Proc. Natl. Acad. Sci. USA*, 2012, **109**, E135–E143.
51. Gao, L., Shao, L., Chen, B.-C. and Betzig, E., 3D live fluorescence imaging of cellular dynamics using Bessel beam plane illumination microscopy. *Nature Protoc.*, 2014, **9**, 1083–1101.
52. Bates, M., Jones, S. A. and Zhuang, X., Stochastic optical reconstruction microscopy (STORM): a method for super resolution fluorescence imaging. *Cold Spring Harbor. Protoc.*, 2013, **8**, 498–520.
53. Shcherbakova, D. M., Sengupta, P., Lippincott-Schwartz, J. and Verkhusha, V. V., Photocontrollable fluorescent proteins for superresolution imaging. *Annu. Rev. Biophys*., 2014, **43**, 303–329.
54. Zhang, M. *et al.*, Rational design of true monomeric and bright photoactivatable fluorescent proteins. *Nature Methods*, 2012, **9**, 727–729.
55. Shroff, H. *et al.*, Dual-colour superresolution imaging of genetically expressed probes within individual adhesion complexes. *Proc. Natl. Acad. Sci. USA*, 2007, **104**, 20308–20313.
56. Tiwari, D. K. and Nagai, T., Smart fluorescent proteins: Innovation for barrier-free superresolution imaging in living cells. *Develop. Growth Differ*., 2013, **55**, 491–507.
57. Huang, B., Bates, M. and Zhuang, X., Super-resolution fluorescence microscopy. *Annu. Rev. Biochem*., 2009, **78**, 993–1016.
58. van de Linde, S. *et al.*, Direct stochastic optical reconstruction microscopy with standard fluorescent probes. *Nature Protoc*., 2011, **6**, 991–1009.
59. Bock, H. *et al.*, Two-colour far-field fluorescence nanoscopy based on photoswitchable emitters. *Appl. Phys. B*, 2007, **88**, 161–165.
60. Cremer, C. *et al.*, Superresolution imaging of biological nanostructures by spectral precision distance microscopy. *Biotechnol. J.*, 2011, **6**, 1037–1051.
61. Betzig, E. *et al.*, Imaging intracellular fluorescent proteins at nanometer resolution. *Science*, 2006, **313**, 1642–1645.
62. Thompson, R. E., Larson, D. R. and Webb, W. W., Precise nanometer localization analysis for individual fluorescent probes. *Biophys. J.*, 2002, **82**, 2775–2783.
63. Dertinger, T., Colyer, R., Iyer, G., Weiss, S. and Enderlein, J., fluctuation imaging (SOFI). *Proc. Natl. Acad. Sci. USA*, 2009, **106**, 22287–22292.
64. Moeyaert, B. and Dedecker, P., pcSOFI as a smart label-based superresolution microscopy technique. *Meth. Mol. Biol*., 2014, **1148**, 261–276.
65. Dedecker, P., Mo, G. C. H., Dertinger, T. and Zhang, J., Widely accessible method for superresolution fluorescence imaging of living systems. *Proc. Natl. Acad. Sci. USA*, 2012, **109**, 10909–10914.
66. Dedecker, P., Duwé, S., Neely, R. K. and Zhang, J., Localizer: fast, accurate, open-source, and modular software package for superresolution microscopy. *J. Biomed. Opt*., 2012, **17**, 126008.
67. Moeyaert, B. *et al.*, Green-to-red photoconvertible dronpa mutant for multimodal super-resolution fluorescence microscopy. *ACS Nano*, 2014, **8**, 1664–1673.
68. Hafi, N. *et al.*, Fluorescence nanoscopy by polarization modulation and polarization angle narrowing. *Nature Methods*, 2014, **11**, 579–584.
69. Lee, S., Yen, J., Lee, A. and Bustamante, C., Counting single photoactivatable fluorescent molecules by photoactivated localization microscopy. *PALM*, 2012, **109**, 2–7.
70. Young, C. L., Raden, D. L., Caplan, J. L., Czymmek, K. J. and Robinson, A. S., Cassette series designed for live-cell imaging of proteins and high-resolution techniques in yeast. 2012, 119–136; doi:10.1002/yea
71. Baker, S. M., Buckheit, R. W. and Falk, M. M., Green-to-red photoconvertible fluorescent proteins: tracking cell and protein dynamics on standard wide-field mercury arc-based microscopes. *BMC Cell Biol*., 2010, **11**, 15.
72. Gurskaya, N. G. *et al.*, Engineering of a monomeric green-to-red photoactivatable fluorescent protein induced by blue light. *Nature Biotechnol*., 2006, **24**, 461–465.
73. Chudakov, D. M., Lukyanov, S. and Lukyanov, K. A., Using photoactivatable fluorescent protein Dendra 2 to track protein movement. *Tech Insight*, 2007, **42**.
74. Falk, M. M., Baker, S. M., Gumpert, A. M., Segretain, D. and Buckheit, R. W., Gap junction turnover is achieved by the internalization of small endocytic double–membrane vesicles. 2009, **20**, 3342–3352.
75. Kural, C., Nonet, M. L. and Selvin, P. R., NIH Public Access. 2010, **48**.
76. Flynn, K. C., Pak, C. W., Shaw, A. E., Bradke, F. and Bamburg, J. R., Growth cone-like waves transport actin and promote axonogenesis and neurite branching. *Dev. Neurobiol*., 2009, **69**, 761–779.

77. Chudakov, D. M., Lukyanov, S. and Lukyanov, K. A., Tracking intracellular protein movements using photoswitchable fluorescent proteins PS-CFP2 and Dendra2. *Nature Protoc.*, 2007, **2**, 2024–2032.
78. Chudakov, D. M. *et al.*, Photoswitchable cyan fluorescent protein for protein tracking. *Nature Biotechnol.*, 2004, **22**, 1435–1439.
79. Zhang, L. *et al.*, Method for real-time monitoring of protein degradation at the single cell level. *Biotechniques*, 2007, **42**, 446–450.
80. Subach, O. M. *et al.*, A photoswitchable orange-to-far-red fluorescent protein, PSmOrange. *Nature Methods*, 2011, **8**, 771–717.
81. Subach, F. V. *et al.*, Photoactivation mechanism of PAmCherry based on crystal structures of the protein in the dark and fluorescent states. *Proc. Natl. Acad. Sci. USA*, 2009, **106**, 21097–21102.
82. Subach, F. V., Patterson, G. H., Renz, M., Lippincott-Schwartz, J. and Verkhusha, V. V., Bright monomeric photoactivatable red fluorescent protein for two-colour super-resolution sptPALM of live cells. *J. Am. Chem. Soc.*, 2010, **132**, 6481–6491.
83. Cella Zanacchi, F. *et al.*, Live-cell 3D super-resolution imaging in thick biological samples. *Nature Meth.*, 2011, **8**, 1047–1049.
84. Ando, R., Mizuno, H. and Miyawaki, A., Regulated fast nucleocytoplasmic shuttling observed by reversible protein highlighting. *Science*, 2004, **306**, 1370–1373.
85. Pletnev, S., Subach, F. V., Dauter, Z., Wlodawer, A. and Verkhusha, V. V., A structural basis for reversible photoswitching of absorbance spectra in red fluorescent protein rsTagRFP. *J. Mol. Biol.*, 2012, **417**, 144–151.
86. Stiel, A. C. *et al.*, Generation of monomeric reversibly switchable red fluorescent proteins for far-field fluorescence nanoscopy. *Biophys. J.*, 2008, **95**, 2989–2997.

Received 17 December 2015; revised accepted 6 September 2016

doi: 10.18520/cs/v112/i04/714-724